Radiotherapy and Oncology 122 (2017) 178–184

Contents lists available at ScienceDirect

Radiotherapy and Oncology

journal homepage: www.thegreenjournal.com

Morbidity of head and neck radiotherapy

Diffusion-weighted magnetic resonance imaging for evaluation of salivary gland function in head and neck cancer patients treated with intensity-modulated radiotherapy

Venla Loimu [a,*], Tiina Seppälä [a], Mika Kapanen [a,b], Laura Tuomikoski [a], Heidi Nurmi [a], Antti Mäkitie [c,d], Mikko Tenhunen [a], Kauko Saarilahti [a]

[a] Helsinki University Central Hospital, Cancer Center, Department of Radiation Oncology; [b] Tampere University Central Hospital, Department of Medical Physics; [c] Helsinki University Central Hospital, Department of Otorhinolaryngology and Head and Neck Surgery, Finland; and [d] Karolinska Institutet, Karolinska University Hospital, Division of Ear, Nose and Throat Diseases, Department of Clinical Sciences, Intervention and Technology, Sweden

ARTICLE INFO

Article history:
Received 6 March 2016
Received in revised form 30 May 2016
Accepted 5 July 2016
Available online 27 July 2016

Keywords:
DW-MRI
IMRT
Salivary glands
Head and neck cancer
Salivary gland scintigraphy
Chemoradiotherapy

ABSTRACT

Background and purposes: Permanent xerostomia as a result of radiation-induced salivary gland damage remains a common side effect of radiotherapy (RT) of the head and neck. The purpose of this study was to evaluate the usefulness of diffusion-weighted magnetic resonance imaging (DW-MRI) in assessing the post-RT salivary gland function in patients with head and neck cancer (HNC).

Materials and methods: In this prospective study, 20 HNC patients scheduled for bilateral neck chemoradiotherapy (CRT) with weekly cisplatin went through diffusion-weighted magnetic resonance imaging (DW-MRI) and salivary gland scintigraphy (SGS) prior to and at a mean of six months after completing the treatment. The changes in apparent diffusion coefficient (ADC) before and after treatment were compared with ejection fraction (EF) measured with SGS and the radiation dose absorbed by the salivary glands.

Results: As a result of gustatory stimulation with ascorbic acid, the ADC showed a biphasic response with an initial increase and subsequent decrease. This pattern was seen both before and after RT. Post-RT ADC increased as a function of RT dose absorbed by the salivary glands. A moderate statistical correlation between pre- and post-RT ADCs at rest and EF measured with SGS was found.

Conclusions: DW-MRI seems a promising tool for detection of physiological and functional changes in major salivary glands after RT.

Radiation-induced salivary gland damage and consequential xerostomia is one of the most common and distressing adverse effects of radiotherapy (RT) for head and neck cancer (HNC) [1–2]. Mechanisms of salivary gland damage related to radiation are incompletely understood [3] and interventions for reducing radiation-induced hyposalivation remain limited. Despite the modern highly conformal intensity modulated radiotherapy or proton therapy (IMRT/IMPT) techniques, sparing of the salivary gland function after RT is not always possible [4–5].

Thus far, salivary gland scintigraphy (SGS) and quantitative salivary flow rate measurements have been the mainstay of assessing the salivary gland function in HNC patients. SGS has shown to be feasible of predicting post-RT salivary gland function [6] but the usefulness of this measurement modality is limited by its invasiveness as well as the radiation exposure related to it. Quantitative salivary flow rate measurements are somewhat unspecific and their results are not always comparable between studies [7].

During the past years, diffusion-weighted magnetic resonance imaging (DW-MRI) has gained increasing interest in assessing various conditions affecting salivary glands [8–16]. As an imaging technique able to show the random thermal molecular diffusion of water molecules (i.e. the Brownian motion) in biological tissues, it characterizes tissues and generates image contrasts based on differences in water mobility. The diffusion leads to signal attenuation, which can be quantified as the apparent diffusion coefficient (ADC). In highly cellular tissues, e.g. tumours, the movement of free water is limited, which leads to decrease in ADC. On the contrary, in hypocellular tissues, e.g. necrosis, the diffusion is high, which can be detected as an increase in ADC [17–18].

DW-MRI's feasibility of assessing salivary gland function has been studied in healthy volunteers [19–21] and in patients with various conditions affecting salivary gland function [10–11] as well

* Corresponding author at: Helsinki University Central Hospital, Cancer Center, PO Box 180, 00029 HUS Helsinki, Finland.
E-mail address: venla.loimu@hus.fi (V. Loimu).

http://dx.doi.org/10.1016/j.radonc.2016.07.008
0167-8140/

as in HNC patients treated with radiotherapy [12–16]. The previous studies have shown that changes in ADC both before and after gustatory stimulation correlate with changes in salivary gland function. Still, in these studies the alterations in ADC before and after RT and responses to salivary stimulation have varied widely, and their clinical relevance remains incompletely understood. Further interpretation is needed to achieve a better understanding of the usability of DW-MRI in this area.

In this prospective study of 20 patients treated with IMRT for head and neck cancer we aimed at evaluating the feasibility of DW-MRI for assessing the post-RT salivary gland function both at rest and in a stimulated state by matching alterations in ADC to radiation dose absorbed by the salivary glands and comparing the results with SGS.

Patients and methods

This prospective study comprises 21 consecutive patients with histologically confirmed squamous cell carcinoma of the head and neck region who were scheduled for bilateral neck IMRT with a curative intent between May 2012 and July 2013. One patient dropped out of the study due to numerous treatment-related complications, resulting in a total of 20 patients included in the analyses. An institutional Research Ethics Board approval was granted for the study, and informed consent was obtained from all patients prior to participation.

The main patient and tumour characteristics are presented in Table 1.

Prior to treatment, the patients went through standard pretreatment evaluation including clinical head and neck examination, imaging (CT/MRI) and endoscopy. All diagnoses were histopathologically confirmed. The tumours were staged according to the 7th UICC TNM classification. All patients had a good performance status (ECOG 0-1) and none of them had any previous salivary gland diseases or other medical causes of xerostomia.

Treatment

All patients received IMRT-based chemoradiotherapy (CRT) with weekly cisplatin 40 mg/m^2. A thermoplastic head and neck mask (Orfit®) was used for immobilization of the patients. Treatment target delineation was based on treatment planning CT and MRI, both performed in the treatment position.

Irradiation was performed with a 6 MV linear accelerator using a dynamic multileaf collimator with the sliding window principle. In all patients the treatment was given with 2 Gy daily fractions up to the planned dose with a mean treatment duration of 49 days (range, 46–56 days). All patients first received 50 Gy to the elective lymph node areas on both sides of the neck as well as to the macroscopic tumour area(s). Thereafter the RT volume was reduced (once in 11 patients and twice in 9 patients) and the high risk/macroscopic tumour areas were boosted up to 60–70 Gy. In 19 of the patients the CRT was given as a definitive treatment with the total prescribed dose up to 70 Gy; the remaining patient went through neck dissection due to recurrent lymph node metastases of a previously operated carcinoma of the soft palatine whereafter she received postoperative CRT up to 60 Gy.

The mean RT dose to the contralateral parotid gland was aimed at being kept <26 Gy whenever feasible. Also the dosage to submandibular glands was tried to be kept as low as reasonably possible.

Table 1
Patient and tumour characteristics.

Male/female, *n* (%)	16 (80%)/4 (20%)
Age, years (mean)	42–74 (59.5)
Tumour site, *n* (%)	
Larynx	1 (5%)
Oropharynx	19 (95%)
Stage, *n* (%)	
I	0 (0%)
II	3 (15%)
III	3 (15%)
IVa	13 (65%)
IVb	1 (5%)
IVc	0 (0%)

MRI protocol

The imaging was performed with a 1.5 T MR scanner GE Optima® MR450w (GE Medical Systems, Milwaukee, WI, USA). MRI scans were made a mean of 8 days (5–15) prior to the treatment onset and a mean of 6 months (with an exception of one patient who underwent imaging already at 3.7 months) after completion of the treatment.

Prior to treatment the routinely used fast recovery fast spin echo T2-weighted (TE = 89 ms, TR = 9400 ms, matrix size = 416 × 224, slice thickness = 3.5 mm, gap = 1.0 mm, FOV = 260 mm) and contrast-enhanced T1-weighted (TE = 3 ms, TR = 17 ms, matrix size = 256 × 256, slice thickness = 2.0 mm, gap = 0, FOV = 280 mm) RT planning images with six channel Neuro Flex coils were first obtained with the patient wearing an immobilization mask. Then the patients were repositioned to a 32-channel head-neck-spine (HNS) coil and their heads were supported with vendor's cushions. For the purposes of this study, T2-weighted imaging with same parameters as above and DW echo-planar imaging (EPI) were performed. In the post-RT scans, only T2 and DWI sequences with the 32-channel HNS coil were included.

Twenty-nine transverse DWI images (TE = 76 ms, TR = 5700 ms, matrix size = 128 × 128, gap = 0 mm, FOV = 260 mm) were obtained with b factors of 0 and 700 s/mm^2 – the latter value was chosen because it was high enough to exclude the contribution from tissue perfusion but low enough to retain high signal intensity level [22]. The slice thickness varied between 3.5–3.9 mm depending on the patient size and was the same in pre- and post-RT imaging. Entire parotid and submandibular glands were included in each of the scans. The constant acquisition time of each DWI sequence was 90 s including the prescanning time of 39 s and without delay the scanning time of 51 s. The first two DWI series were acquired at rest, whereafter the patients were given two 500 mg tablets of ascorbic acid orally. For salivary stimulation, the patients were advised to bite the tablets. Then, the DWI sequence was repeated a mean of ten times.

ADC maps were saved in the AW® workstation (version 4.6, GE Medical Systems, Milwaukee, WI, USA) using READY View® software, and EPI correction was applied to remove EPI distortions. The ADCs were calculated from the equation: $S(i) = S_0 \times \exp(-b_i \times \mathrm{ADC})$ where $S(i)$ is the signal intensity measured on the ith b value image, b_i is the corresponding b value, and S_0 is the exact signal intensity for $b = 0$ s/mm^2. For DWI analysis, the data were transferred from the AW workstation to the image processing software (MIM 5.6, MIM Software Inc., Cleveland, OH, USA). The ADC was measured on ADC maps using regions of interest (ROIs) placed over each of the salivary glands. For this purpose, all of the salivary glands were manually delineated on DWI sequences, and for anatomical reference also on T2-weighted images. Large vessels, such as the retromandibular vein and the external carotid artery were excluded. DWI scans of each patient were manually registered to each time series to minimize the interpretation bias caused by the geometric distortion in EPI DWI images.

Scintigraphy

All patients underwent salivary scintigraphy at a mean of 3 days prior to the treatment onset (range, 11 days prior to – 5 days after) and a mean of 6 months after completing the treatment (one patient underwent SGS already at 3.5 months after the treatment). Dynamic ^{99m}Tc pertechnetate (185 MBq) imaging was performed using Siemens Symbia® T2 gamma camera, and a lemon juice bolus was used to stimulate saliva excretion after 15 min of imaging. The imaging procedure is described elsewhere [6]. For the calculation of salivary ejection fraction (sEF) the four major salivary glands were segmented in the dynamic image series, resulting in four time-activity curves. An additional ROI was contoured for background correction. The sEF was calculated using equation

$$\mathrm{sEF} = \frac{C_{\max} - C_{\min}}{C_{\max} - C_{\mathrm{bg}}}$$

where $C_{\max}$ and $C_{\min}$ are the detected counts in the salivary gland ROI immediately before and after the stimulus, respectively, and C_{bg} are the counts in the background ROI. The relative ejection fraction (rEF) was calculated from rEF(t) = sEF(t)/sEF(0), where sEF(t) was defined six months after RT and sEF(0) was the baseline value measured before RT.

Statistical analysis

SPSS Statistics software was used for the statistical analyses. The normality of the data was confirmed using Kolmogorov–Smirnov and Shapiro–Wilk-tests. *T*-test and Wilcoxon Signed Ranks test were used to compare different ADC values. *P*-values of <0.05 were considered statistically significant.

The data in the graphs were divided into subgroups of equal sizes to demonstrate dependence pattern between the compared parameters. Pearson correlation coefficient was calculated to investigate the dependence between dose, ADC and scintigraphy parameters.

Results

High-quality MRI scans were obtained for all patients. In all patients, both of the parotid glands appeared normal in the T1 and T2 sequences, resulting in a total of 40 examined parotid glands. On the contrary, one patient had only one submandibular gland and one patient was lacking both of them, resulting in 37 examined submandibular glands.

The mean total RT doses to the right and left parotid glands were 30.2 Gy (range, 19.5–47.7 Gy) and 37.4 Gy (21.7–55.9 Gy), respectively. The corresponding doses to the right and left submandibular glands were 46.3 Gy (27.0–68.1 Gy) and 59.6 Gy (36.7–70.4 Gy).

Baseline ADC (10^{-3} mm^2/s, mean ± SD) at rest (i.e. in prestimulated glands) was higher in submandibular glands (1.35 ± 0.09) than in parotid glands (1.15 ± 0.12) ($p < 0.001$). The corresponding post-RT values for submandibular and parotid glands in an unstimulated state were 1.73 ± 0.22 and 1.48 ± 0.16 respectively (Table 2). This increase in ADC values after RT was statistically significant ($p < 0.001$) for both parotid and submandibular glands.

After salivary stimulation with ascorbic acid, an initial increase and subsequent decrease in ADC was seen in both parotid and submandibular glands. This pattern of response to salivary stimulation was present both pre and post RT. The maximum ADC value after stimulation (ADC_{max}) was significantly higher in irradiated glands (post-RT) compared with the non-irradiated ones (pre-RT) ($p < 0.001$). Also the change from baseline to the ADC_{max} was significantly higher in the post-RT setting compared with the pre-RT one ($p < 0.01$) (Table 2).

We also found a linear correlation between the RT dose absorbed by the salivary glands and pre- and post-RT changes in ADC ($ADC_{post-pre}$) (Fig. 1). This dose–response relationship was seen in both parotid and submandibular glands in the prestimulated state ($p < 0.001$) as well as in the first ADC registration point after salivary stimulation.

Fig. 2 depicts the pre- and post-RT ADC histograms of a single patient's salivary glands at rest. Here, considering each of the salivary glands separately, it is seen that the ADC values inside the salivary glands are normally distributed, and that in the glands that absorbed a high RT dose, the ADC distribution after RT is shifted to right whereas no noticeable change is seen in the glands that received a low RT dose.

Scintigraphy

Salivary scintigraphy was performed for all patients before and after treatment. Three parotid and 9 submandibular glands showed no measurable pretreatment function, and one post treatment measurement failed because the patient's head was moving during the measurement. The glands whose activity was failed to be measured were excluded from the analysis. This resulted in a total of 35 examined parotid glands and 30 examined submandibular glands.

Relative ejection fraction (rEF), defined as the ratio of the salivary ejection fraction after and before treatment, decreased as a function of the mean RT dose absorbed by the salivary glands; this was in accordance with our previously reported results [6].

The relationship between pre- and post-RT changes in baseline ADCs and rEFs is presented in Fig. 3. When matching prestimulated $ADC_{post-pre}$ values and rEFs for all of the examined salivary glands ($n = 65$), a modest correlation ($r = -0.38$, $p < 0.01$) was found. When regarding the parotid and submandibular glands separately, the corresponding correlations were $r = -0.29$, $p < 0.1$ and $r = -0.50$, $p < 0.01$, respectively.

The temporal relationship between SGS and DWI measurements is schematically presented in Fig. 4 (Suppl data). Here, it is visualized that the peak salivary gland technetium intake right before the activity drop in SGS corresponds to the baseline ADC in DW-MRI. The time gap between the moment when the patient bites the ascorbic acid tablets and when post-stimulation DWI measurements are started to be made is estimated to be about 25 s. Thus, the post-stimulation DWI series correspond to the time after the activity drop in SGS has already happened. DW and SGS images on an example patient before RT are presented in Fig. 5 (Suppl data).

Discussion

In this prospective study we characterized the pre- and post-RT distribution of ADC values in salivary glands at rest and in a stimulated state. These results were compared with SGS. Our main findings were the increase of $ADC_{post-pre}$ values as a function of the RT dose absorbed by the salivary glands in both prestimulated and stimulated states and the moderate statistical correlation between prestimulated $ADC_{post-pre}$ values and rEFs measured by SGS. In this study we also confirmed some of the previously reported data about the DW-MRI and SGS.

In previously published articles [10–11,14–15,19–20] of patients and healthy volunteers, the pattern of response to gustatory stimulation in DW-MRI and changes in the ADC as a result of RT to the salivary glands have varied considerably. The correlation between changes in ADC and clinical parameters, such

Table 2
Summary of the measurement characteristics.

Mean ± 1SD	PG, right	PG, left	PG, both	SMG, right	SMG, left	SMG, both
D_{mean}, Gy	30.2 ± 8.8	37.4 ± 10.6	33.8 ± 10.3	46.3 ± 14.2	59.6 ± 12.3	52.7 ± 14.7
EF_{pre}, %	44.4 ± 17.1	43.5 ± 16.0	44.0 ± 16.3	35.4 ± 13.9	29.8 ± 16.6	32.7 ± 15.3
EF_{post}, %	29.1 ± 18.6	26.9 ± 20.3	28.0 ± 19.3	16.1 ± 14.2	4.9 ± 7.9	10.7 ± 12.8
rEF, %	64.0 ± 37.1	56.9 ± 46.0	60.5 ± 41.2	52.3 ± 43.6	22.6 ± 31.5	37.9 ± 40.5
$ADC_{base,\ pre}$, ($\times 10^{-3}$)	1.15 ± 0.11	1.14 ± 0.13	1.15 ± 0.12	1.34 ± 0.09	1.37 ± 0.10	1.35 ± 0.09
$ADC_{stim1,\ pre}$, ($\times 10^{-3}$)	1.38 ± 0.16	1.38 ± 0.23	1.38 ± 0.20	1.70 ± 0.22	1.68 ± 0.27	1.69 ± 0.24
$ADC_{max,\ pre}$, ($\times 10^{-3}$)	1.43 ± 0.14	1.42 ± 0.21	1.42 ± 0.18	1.79 ± 0.18	1.80 ± 0.25	1.79 ± 0.21
$T_{max,\ pre}$, s	158 ± 82	144 ± 79	151 ± 80	156 ± 73	155 ± 92	156 ± 81
$ADC_{base,\ post}$, ($\times 10^{-3}$)	1.44 ± 0.17	1.52 ± 0.15	1.48 ± 0.16	1.66 ± 0.21	1.81 ± 0.20	1.73 ± 0.22
$ADC_{stim1,\ post}$, ($\times 10^{-3}$)	1.69 ± 0.23	1.81 ± 0.25	1.75 ± 0.24	2.00 ± 0.30	2.28 ± 0.34	2.14 ± 0.35
$ADC_{max,\ post}$, ($\times 10^{-3}$)	1.76 ± 0.20	1.87 ± 0.28	1.82 ± 0.25	2.21 ± 0.22	2.49 ± 0.42	2.35 ± 0.36
$T_{max,\ post}$, s	198 ± 126	185 ± 126	191 ± 124	223 ± 142	235 ± 139	229 ± 138

PG = parotid gland, SMG = submandibular gland, D_{mean} = mean absorbed dose, EF_{pre} = ejection fraction before RT, EF_{post} = ejection fraction 6 months after RT, rEF = EF_{post}/EF_{pre}, $ADC_{base,\ pre}/ADC_{base,post}$ = baseline ADC before/after RT, $ADC_{stim1,\ pre}/ADC_{stim1,\ post}$ = ADC in the first measurement point after gustatory stimulation before/after RT, $ADC_{max,\ pre}/ADC_{max,\ post}$ = maximum ADC value after gustatory stimulation before/after RT, $T_{max,\ pre}/T_{max,\ post}$ = Time to ADC_{max} before/after RT.

as subjective xerostomia and absolute salivary flow rates remains unclear. Further, the relationship between RT dose to the salivary glands and changes in ADC or the correlation between pre and post RT changes in ADC and rEFs have not previously been proven.

In this series, the baseline ADC at rest was significantly higher in submandibular than in parotid glands. This finding is in accordance with previous studies [15,19] and it is thought to reflect the higher proportional amount of extracellular water of the submandibular glands [15]. Also most of the previously published studies reported the post-RT rise in ADC values of prestimulated glands using high *b* values [12–15]. This rise is thought to reflect the increased water diffusivity in the damaged salivary glands as a result of cellular loss, fibrosis or both [15].

In the present study, the gustatory stimulation with two 500 mg tablets of ascorbic acid resulted in a significant rise in ADC values of unirradiated glands. According to the previous reports, the pattern of response to gustatory stimulation in non-irradiated glands has varied widely. This may contribute to the *b*-values chosen (lower *b* values are more sensitive to perfusion whereas higher b values detect the actual diffusion, [22–23]) and – perhaps more importantly – the used stimulating agent. In their studies Thoeny [19] and Dirix [15] used a 500 mg tablet of ascorbic acid as the stimulating agent and advised the patients to let the tablet dissolve in their mouths, not to chew on it. This resulted in an initial decrease and subsequent increase in the ADC values. Meanwhile, Habermann [20], Ries [10], Kato [11] – having used lemon juice as a stimulant – and Zhang [14] – who performed the gustatory stimulation with six tablets of 100 mg of ascorbic acid – reported an initial increase and subsequent fluctuation in the ADC values. This pattern of response to gustatory stimulation was also seen in our study. This may be explained by the quicker saliva production as a response to more immediate stimulation [14]: lemon juice, higher number of tablets of ascorbic acid or two instantly bitten tablets of ascorbic acid are likely to stimulate simultaneously more receptors than a single slowly dissolving tablet of ascorbic acid does.

When regarding the post-RT state, this pattern of response to gustatory stimulation still existed in our patients, suggesting a persisting capacity of the acinar cells to produce saliva upon stimulation [14]. Also the range of increase of the ADC values was higher in irradiated glands compared with the non-irradiated ones, suggesting a greater increase of free water in the extracellular space. As Zhang et al. [14] suggested, this may be due to delayed saliva emptying due to damaged salivary duct system after RT. A similar post-RT response to gustatory stimulation was reported by Zhang et al. in 28 patients with nasopharyngeal carcinoma at 2 weeks after finishing the treatment [16]. On the contrary, in their series of 8 patients with HNC, Dirix et al. reported a loss of the pre-RT pattern of response to gustatory stimulation in non-functional glands at 9 months after finishing the RT [15]. This difference may partly be attributable to the different kind of salivary stimulation.

The relationship between the RT dose to the salivary glands and changes in ADC in the unstimulated state has previously been investigated by Doornaert [12] and Marzi [13]. In their series of 34 patients, Marzi et al. found a correlation between the RT dose to the parotid glands and pure diffusion coefficient ($r = 0.197$, $p = 0.046$) and parotid shrinkage ($p = 0.010$) when data from measurement points at half way through and at the end of RT were taken into account. No significant correlation between ADC changes and parotid RT dose was reported. Meanwhile, in their small study of 8 patients with HNC, Doornaert et al. found a better correlation between RT dose absorbed by the salivary glands and changes of ADC at certain ROIs of the salivary glands when using HASTE technique ($r = 0.33$) than when using the EPI technique ($r = 0.11$) at 2–3 months after finishing the RT. Still, to our knowledge, our study was the first one to confirm a dose–response relationship in ADC changes in a longer term follow up. The increase in ADC as a result of RT damage was evident in irradiated salivary glands – the more clearly the higher the RT dose was. This dependency was more clearly evident in submandibular glands compared with the parotid glands, probably due to the higher RT dose absorbed by submandibular glands. Further, the dose–response correlation was also present in the stimulated state – even though weaker than in the pre-stimulated state. This weaker correlation in stimulated salivary glands may partly be due to uncertainties related to salivary gland stimulation procedure.

Finally, we analysed the correlation between $ADC_{post-pre}$ and rEF. This correlation was more evident in submandibular glands ($r = -0.50$, $p < 0.01$) compared with parotid glands ($r = -0.29$, $p < 0.1$). The stronger correlation coefficient in submandibular glands may partly be explained by higher RT dose absorbed by these glands. Correlating these two modalities with each other is difficult, as SGS and DW-MRI do not measure exactly the same things. While DW-MRI depicts the movement of water molecules in the salivary gland tissue and does not directly reflect the secretory function, the Tc99 m pertechnetate uptake in SGS reflects the parenchymal function and the output reflects the secretory function (Fig. 4). However, this correlation suggests that there is a clinical relevance in changes in ADC in terms of decreased salivary gland output. In this study, no absolute of subjective xerostomia was assessed. However, in our previous studies [6,30] we have shown a clear correlation between absolute salivary flow rates ad EF measured with SGS, which further confirms the clinical relevance of this finding.

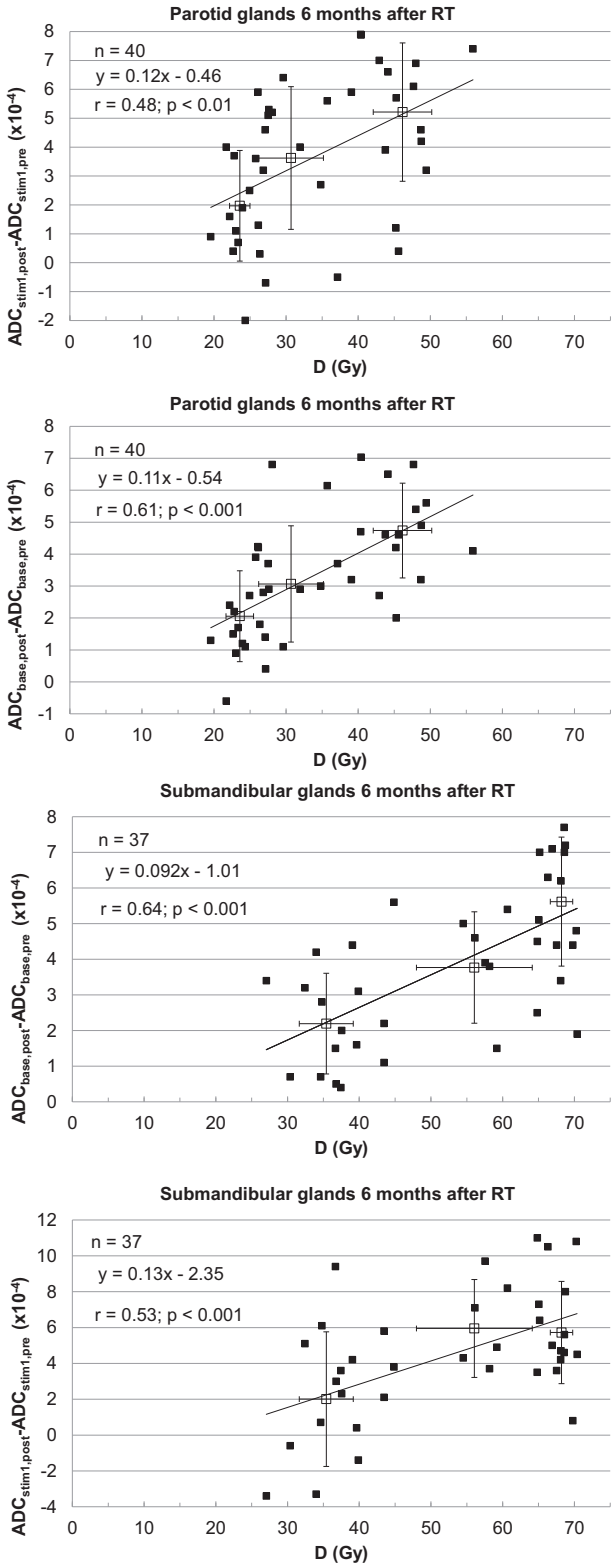

Fig. 1. The change of ADC values ($ADC_{post-pre}$) in pre- and post-stimulated states as a function of RT dose absorbed by the salivary glands.

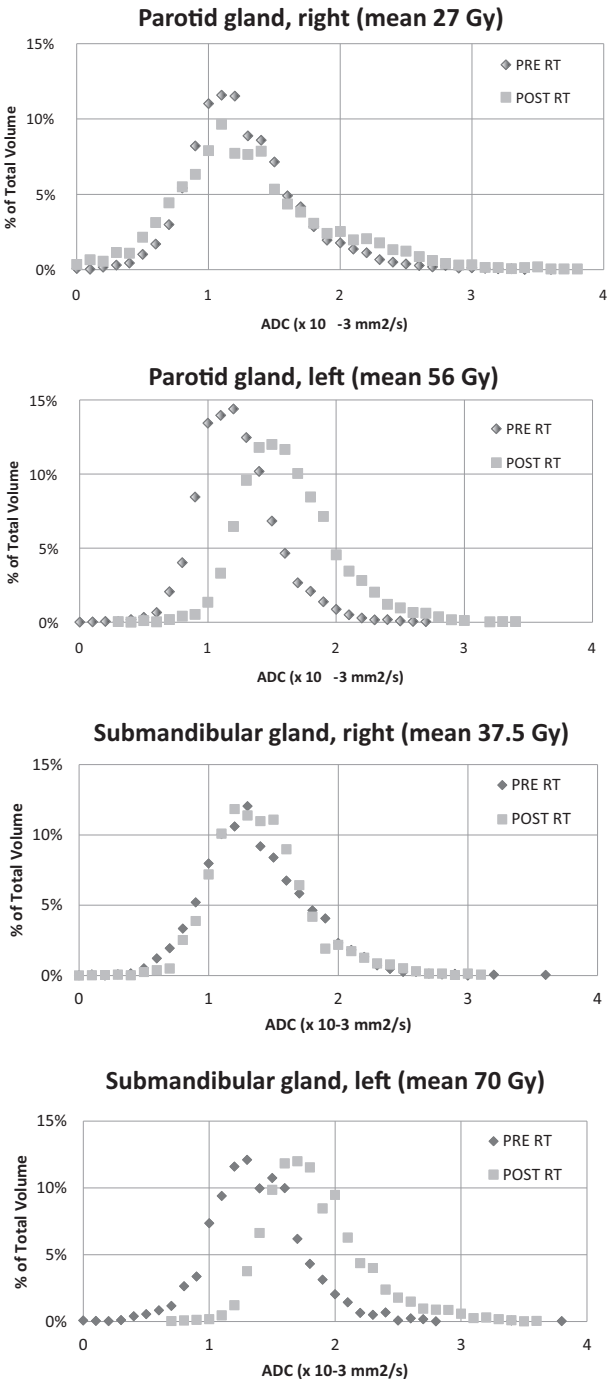

Fig. 2. A single-patient example of ADC histograms of pre-stimulated salivary glands before and at six months after RT.

There are some limitations that should be pointed out: First, the number of patients was relatively small which may make the statistics difficult to interpret. Second, imaging technique and equipment may contribute to the results. Not all of the salivary glands could be analysed with SGS due to inability to measure their function. The time gap between the patient biting the tablet of ascorbic acid and the initiation of DW imaging varied between 5 and 50 s. This delay may have caused some inaccuracies in measuring of the ADC values in the stimulated state. Further, only one b factor in addition to zero could be used in this study. It was chosen to be 700 to allow decently high resolution while excluding the perfusion component. Use of more than two b values would possibly have led to different changes in ADC. In addition, EPI scans, especially with high b-values, are prone to notable geometric distortions. To minimize the uncertainty caused by this distortion, we registered each time series manually to the scans. Finally, earlier publications [3,24] have reported on regional differences in

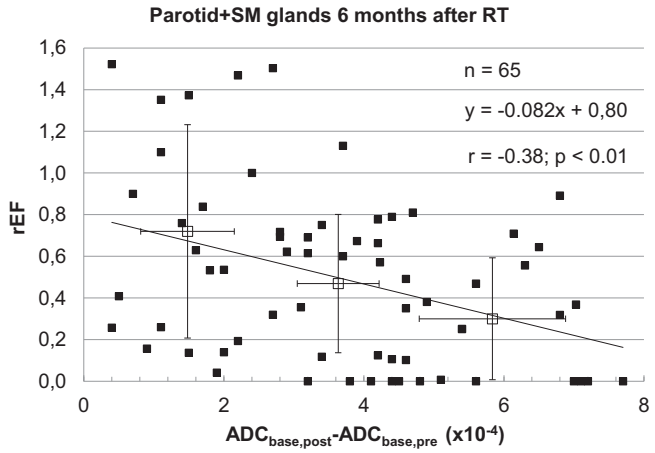

Fig. 3. The relationship between relative ejection fraction (rEF) and change of baseline ADC values in all salivary glands.

radiosensitivity inside the salivary glands. According to them, it is suggested that acinic cell progenitors are located exclusively within the parotid ducts, particularly the larger ones, and that irradiating these regions to high doses is very likely to cause irreversible xerostomia due to RT-induced stem cell loss and consequential inability of the salivary glands to regenerate. Since the present study was performed primarily to compare DW-MRI with SGS, and since the regional resolution in planar SGS scans is poor, no specific dose distribution inside the salivary glands and its correlations to measurement parameters could be analysed.

Over the past decade, the role of diffusion weighted MR imaging in patients with HNC has gained increasing interest. In addition to the increasing understanding of its capability to depict physiological and functional changes in salivary glands after RT, it has also proven to be a promising tool for tissue characterization, nodal staging and early response evaluation in this patient group [25–29].

Until recently, evaluation of the salivary gland function in this patient group has been based on SGS. However, the use of this measurement modality is limited by the radiation exposure related to it as well as lack of resolution in planar images to allow regional assessment of the salivary gland function. With DW-MRI, better information on regional changes inside the salivary glands could be achieved without additional radiation exposure. As the DWI scans take only a few minutes to obtain in addition to the routinely used planning-MRI sequences, this is also much more convenient to the patients. Since our aim would be to use more adaptive treatment strategies for these patients in the future, adding DW sequences routinely to planning-MR scans could give more detailed information not only on anatomical structures and early tumour response but also on salivary gland function, thus allowing the possibility to adjust the treatment plan accordingly.

Conclusions

Our results showed that Post-RT changes in ADC correlate with RT dose absorbed by the salivary glands and rEF measured by SGS, suggesting that DW-MRI could be a useful tool for detection of radiation-induced physiological and functional changes in the major salivary glands in HNC patients. More investigation is needed to fully understand the optimal way of using DW imaging in the assessment of salivary gland function in this patient group.

Conflicts of interest

None.

Acknowledgements

This study has been supported by grants from the Helsinki University Hospital Research Funds.

Appendix A. Supplementary data

Supplementary data associated with this article can be found, in the online version, at http://dx.doi.org/10.1016/j.radonc.2016.07.008.

References

[1] Beetz I, Steenbakkers RJ, Chouvalova O, et al. The QUANTEC criteria for parotid gland dose and their efficacy to prevent moderate to severe patient-rated xerostomia. Acta Oncol 2014;53:597–604.
[2] Jellema AP, Slotman BJ, Doornaert P, Leemans CR, Langendijk JA. Impact of radiation-induced xerostomia on quality of life after primary radiotherapy among patients with head and neck cancer. Int J Radiat Oncol Biol Phys 2007;69:751–60.
[3] Vissink A, van Luijk P, Langendijk J, Coppes R. Current ideas to reduce or salvage radiation damage to salivary glands. Oral Dis 2015;21:e1–e10.
[4] Nutting CM, Morden JP, Harrington KJ, et al. Parotid-sparing intensity modulated versus conventional radiotherapy in head and neck cancer (PARSPORT): a phase 3 multicentre randomised controlled trial. Lancet Oncol 2011;12:127–36.
[5] Jakobi A, Bandurska-Luque A, Stützwe K, et al. Identification of patient benefit from proton therapy for advanced head and neck cancer patients based on individual and subgroup normal tissue complication probability analysis. Int J Radiat Oncol Biol Phys 2015;92:1165–74.
[6] Tenhunen M, Collan J, Kouri M, et al. Scintigraphy in prediction of the salivary gland function after gland-sparing intensity modulated radiation therapy for head and neck cancer. Radiother Oncol 2008;87:260–7.
[7] Eisbruch A, Rhodus N, Rosenthal D, et al. How should we measure and report radiotherapy-induced xerostomia? Semin Radiat Oncol 2003;13:226–34.
[8] Patel RR, Carlos RC, Midia M, et al. Apparent diffusion coefficient mapping of the normal parotid gland and parotid involvement in patients with systemic connective tissue disorders. Am J Neuroradiol 2004;25:16–20.
[9] Yoshino N, Yamada I, Ohbayashi N, et al. Salivary glands and lesions: evaluation of apparent diffusion coefficients with split-echo diffusion-weighted MR-imaging—initial results. Radiology 2001;221:837–42.
[10] Ries T, Arndt C, Regier M, et al. Value of apparent diffusion coefficient before and after gustatory stimulation in the diagnosis of acute or chronic parotitis. Eur Radiol 2008;18:2251–7.
[11] Kato H, Kanematsu M, Toida M, et al. Salivary gland function evaluated by diffusion-weighed MR imaging with gustatory stimulation: preliminary results. J Magn Reson Imaging 2011;34:904–9.
[12] Doornaert P, Dahele M, Ljumanovic R, De Bree R, Slotman BJ, Castelijns JA. Use of diffusion-weighted magnetic resonance imaging (DW-MRI) to investigate the effect of chemoradiotherapy on the salivary glands. Acta Oncol 2015;54:1068–71.
[13] Marzi S, Forina C, Marucci L, et al. Early radiation-induced changes evaluated by intravoxel incoherent motion in the major salivary glands. J Magn Reson Imaging 2015;41:974–82.
[14] Zhang Y, Ou D, Gu Y, et al. Diffusion-weighted MRI of salivary glands with gustatory stimulation: comparison before and after radiotherapy. Acta Radiol 2013;54:928–33.
[15] Dirix P, De Keyzer F, Vandecaveye V, Stroobants S, Hermans R, Nuyts S. Diffusion-weighted magnetic resonance imaging to evaluate major salivary gland function before and after radiotherapy. Int J Radiat Oncol Biol Phys 2008;71:1365–71.
[16] Zhang L, Murata Y, Ishida R, Ohashi I, Yoshimura R, Shibuya H. Functional evaluation with intravoxel incoherent motion echo-planar MRI in irradiated salivary glands: a correlative study with salivary gland scintigraphy. J Magn Reson Imaging 2001;14:223–9.
[17] Parker GJM. Analysis of MR diffusion weighted images. Br J Radiol 2004;77:S176–85.
[18] Bammer R. Basic principles of diffusion-weighted imaging. Eur J Radiol 2003;45:169–84.
[19] Thoeny H, De Keyzer F, Claus F, Sunaert S, Hermans R. Gustatory stimulation changes the apparent diffusion coefficient of the parotid glands: initial experience. Radiology 2005;235:629–34.
[20] Habermann CR, Gossrau P, Kooijman H, et al. Monitoring of gustatory stimulation of salivary glands by diffusion-weighted MR imaging: comparison of 1.5T and 3T. Am. J Neuroradiol 2007;28:1547–51.
[21] Juan CJ, Chang HC, Hsueh CJ, et al. Salivary glands: Echo-planar versus propeller diffusion-weighted MR imaging for assessment of ADCs. Radiology 2009;253:144–52.
[22] Thoeny H, De Keyzer F, Boesch C, et al. Diffusion-weighted imaging of the parotid gland: Influence of the choice of b-values on the apparent diffusion coefficient value. J Magn Reson Imaging 2004;20:786–90.

[23] Le BD, Breton E, Lallemand D, et al. Separation of diffusion and perfusion in intravoxel incoherent motion MR imaging. Radiology 1988;164:497–505.
[24] van Luijk P, Pringle S, Deasy JO, et al. Sparing the region of the salivary gland containing stem cells preserves saliva production after radiotherapy for head and neck cancer. Sci Transl Med 2015;7:305ra147.
[25] Srinivasan A, Dvorak R, Perni K, Rohrer S, Mukherji SK. Differentiation of benign and malignant pathology in the head and neck using 3T apparent diffusion coefficient values: early experience. Am J Neuroradiol 2008;29:40–4.
[26] Vandecaveye V, De Keyzer F, Vander Poorten V, et al. Head and neck squamous cell carcinoma: value of diffusion-weighted MR imaging for nodal staging. Radiology 2009;251:134–46.
[27] Schouten CS, de Bree R, van der Putten L, et al. Diffusion-weighted EPI- and HASTE-MRI and 18F-FDG-PET-CT early during chemoradiotherapy in advanced head and neck cancer. Quant Imaging Med Surg 2014;4:239–50.
[28] Vandecaveye V, Dirix P, De Keyzer F, et al. Predictive value of diffusion-weighted magnetic resonance imaging during chemoradiotherapy for head and neck squamous cell carcinoma. Eur Radiol 2010;20:1703–14.
[29] Kim S, Loevner L, Quon H, et al. Diffusion weighted MRI for predicting and detecting early response to chemoradiation therapy of squamous cell carcinomas of the head and neck. Clin Cancer Res 2009;15:986–94.
[30] Tuomikoski L, Kapanen M, Collan J, et al. Toward a more patient-specific model of post-radiotherapy saliva secretion for head and neck cancer patients. Acta Oncol 2015;54:1310–6.